Journal of Southeast University (English Edition) Vol. 21, No. 2, pp. 207－210 June 2005 ISSN 1003—7985

Accelerating SAGE algorithm in PET image reconstruction by rescaled block-iterative method

Zhu Hongqing Shu Huazhong Zhou Jian Luo Limin

(Department of Biological Science and Medical Engineering, Southeast University, Nanjing 210096, China)

Abstract: A new method to accelerate the convergent rate of the space-alternating generalized expectation-maximization (SAGE) algorithm is proposed. The new rescaled block-iterative SAGE (RBI-SAGE) algorithm combines the RBI algorithm with the SAGE algorithm for PET image reconstruction. In the new approach, the projection data is partitioned into disjoint blocks; each iteration step involves only one of these blocks. SAGE updates the parameters sequentially in each block. In experiments, the RBI-SAGE algorithm and classical SAGE algorithm are compared in the application on positron emission tomography (PET) image reconstruction. Simulation results show that RBI-SAGE has better performance than SAGE in both convergence and image quality.

Key words: positron emission tomography; space-alternating generalized expectation-maximization; image reconstruction; rescaled block-iterative; maximum likelihood

The expectation maximization maximum likelihood (EMML) algorithm has been found to produce good reconstruction results, but it has an extremely slow rate of convergence and thus a large number of iterations may be required to yield an acceptable image. A variety of methods have been proposed for accelerating the EM algorithm. One popular and effective method to speed up the reconstruction process is the ordered subset EM (OSEM) method proposed by Hudson and Larkin[1]. They proved the OSEM convergence for a special case, in which the chosen subsets satisfied the restrictive "subset balanced" condition. Byrne developed a rescaled block-iterative version of EMML (RBI-EMML)[2]. It is an accelerated block-iterative version of EMML that converges, in the consistent case, to a solution, for any choice of subsets (blocks). The space-alternating generalized expectation-maximization (SAGE) algorithm proposed by Fessler and Hero[3] is another way to overcome the shortcomings of the EM algorithm. It is based on the fact that hidden-data spaces used by SAGE have less information than the conventional complete-data space, thus yielding a significant improvement in convergence rate. In addition, SAGE updates the parameters sequentially, which makes its M-step be treated easily.

In this paper, a novel algorithm, namely BRI-SAGE that combines RBI algorithm with SAGE algorithm is proposed for PET image reconstruction. In the new approach, the data is partitioned into disjoint blocks, each iteration step involves only one of these blocks. If there is only one block which contains all the data, RBI-SAGE reduces to the SAGE. Some experimental results are provided to illustrate the effectiveness of the proposed algorithm.

Received 2004-10-27.

Foundation item: The National Basic Research Program of China (973 Program) (No. 2003CB716102).

Biographies: Zhu Hongqing (1967—), female, doctor; Shu Huazhong (corresponding author), male, professor, shu. list@ seu. edu. cn.

1 Review of Relevant Algorithms

In emission tomography, according to the assumption that the observed photon counts are independent Poisson random variables over the region of interest[4], we have

$$Y_i = \sum_j N_{ij} + R_i \sim \text{Poisson}\left\{\sum_j p_{ij}x_j + r_i\right\} \quad (1)$$

where Y_i denotes the i-th detector recording emissions which include the photon counts emitted by all pixels and the numbers of emissions brought by background events. $\{R_i\}$ are also independent Poisson variables: $R_i \sim \text{Poisson}\{r_i\}$. Background rates $\{r_i\}$ are assumed to be known. The element of system matrix p_{ij} represents the probability that an emission from pixel j is recorded at detector i. x_j is the expected value of pixel j. The log-likelihood for this problem is given by

$$L(\boldsymbol{x}) = \log f(\boldsymbol{y};\boldsymbol{x}) = \sum_i (y_i \log \bar{y}_i(\boldsymbol{x}) - \bar{y}_i(\boldsymbol{x})) \quad (2)$$

$$\bar{y}_i(\boldsymbol{x}) = \sum_j p_{ij}x_j + r_i \quad (3)$$

Thus, the EM algorithm[5], starting with a strictly positive vector $\boldsymbol{x}^{(1)}$, is written as

$$x_j^{(k+1)} = x_j^{(k)} e_j(\boldsymbol{x}^{(k)}) \Big/ \sum_i p_{ij} \quad (4)$$

$$e_j(\boldsymbol{x}^{(k)}) = \sum_i p_{ij} y_i \Big/ \bar{y}_i(\boldsymbol{x}^{(k)}) \quad (5)$$

where k is the iterative number. Under the assumption of $\{r_i\}$ being zero, the iterative step for the RBI-EM algorithm can be written as follows[6]:

$$x_j^{(k+1)} = x_j^{(k)} + \tau_t (x_j^{(k)} / \sum_i p_{ij}) \sum_{i \in S_t} p_{ij} (y_i / \sum_l p_{il} x_l^{(k)} - 1) \tag{6}$$

where the rescaling factor τ_t for the t-th block S_t, $t = 1, 2, \ldots, n$, is given by

$$\tau_t = \min_j (\sum_i p_{ij} / \sum_{i \in S_t} p_{ij}) \tag{7}$$

From the RBI-EMML algorithm described above, it can be seen that RBI-EMML reduces to OS-EM when the restrictive "subset balances" condition holds. It is demonstrated that the RBI-EM algorithm converges to the correct solution for any choice of subset (block) in the consistent case for linear equation $\boldsymbol{y} = \boldsymbol{Px}$. On the contrary, the RBI-EM produces a limited cycle, how distant from one another the vectors of the limited cycle depend on how large the minimum value of KL($\boldsymbol{y}$, $\boldsymbol{Px}$) is[7]. Here KL($\boldsymbol{y}$, $\boldsymbol{Px}$) is the Kullback-Leibler distance, defined for nonnegative vectors $\boldsymbol{y}$ and $\boldsymbol{Px}$ by

$$\mathrm{KL}(\boldsymbol{y}, \boldsymbol{Px}) = \sum_{i=1}^{I} (y_i \log(y_i / (\boldsymbol{Px})_i) + (\boldsymbol{Px})_i - y_i) \tag{8}$$

where $(\,)_i$ denotes the i-th component of the vector.

2 RBI-SAGE Algorithm

Both the OS algorithm and the RBI algorithm are useful methods to speed up the image reconstruction for EMML. But the "subset balance" condition that the OS algorithm should satisfy is not necessary for the RBI algorithm. This is one of the reasons that we choose the RBI for accelerating SAGE algorithm. The SAGE algorithm was described in detail in Refs. [8, 9]. The RBI-SAGE method we discuss here does not require much time in each iterative step compared with the SAGE algorithm; moreover it needs few iteration steps. Thus, it can reduce significantly the computation time in the reconstruction process. The RBI-SAGE algorithm can be outlined as follows.

Let S_t, $t = 1, 2, \ldots, n$, be a block (not joint), where ns is the block number.

Initialization: Let $\hat{\boldsymbol{x}}^{(1)}$ be a positive starting image vector.

For $k = 1, 2, \ldots$ until convergence of $\hat{\boldsymbol{x}}^{(k)}$, where $\hat{\boldsymbol{x}}^{(k)}$ denotes the estimate of $\boldsymbol{x}$ after k iterations.

For $t = 1, 2, \ldots, n$ (loop on blocks)

For a given block, setup a start image vector: $\boldsymbol{x}^{(k)} = \hat{\boldsymbol{x}}^{(t)}$.

For a given block and a start image vector, calculate the initial projection:

$$\bar{y}_i^t = \sum_j p_{ij} x_j^{(k)} + r_i^t \qquad i \in S_t; j = 1, 2, \ldots, J$$

where J is the dimension of image space.

For $l = 1, 2, \ldots, J$ (loop on image space)

E-step: $e = y_i^t / \bar{y}_i^t - 1$, $e_l^t = \sum_i p_{il} e$

M-step:
$$\begin{cases} \tau_t = \min_l (\sum_i p_{il} / \sum_{i \in S_t} p_{il}) \\ x_l^{(k+1)} = x_l^{(k)} + \tau_t (x_l^{(k)} e_l^t / \sum_i p_{il}) \\ x_q^{(k+1)} = x_q^{(k)} \qquad q \neq l \end{cases}$$

Update: $\bar{y}_i^t = \bar{y}_i^t + (x_l^{(k+1)} - x_l^{(k)}) p_{il} \qquad \forall\, i, a_{il} \neq 0$

Endfor

For the next block, we take $\hat{\boldsymbol{x}}^{t+1} = \boldsymbol{x}^{(k+1)}$

Endfor

Endfor

3 Experimental Results

Some reconstructed results using SAGE and RBI-SAGE are presented to illustrate the effectiveness of these algorithms. Fig. 1 shows the phantom used in our experiment. The relative activities of the elements are shown in Fig. 1. The total photon count of the projection data is 10^6. The sinogram has 128 radial bins and 180 angles. The size of a pixel is 6 mm × 6 mm and the size of the image matrix is 384 mm × 384 mm. The reconstructed images are 64 × 64 pixel matrices. The projection data, including 25% uniform Poisson background noise, is calculated, and the reconstructed images are shown in Fig. 2.

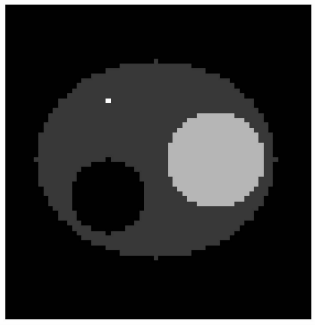

Fig. 1 A simulated phantom

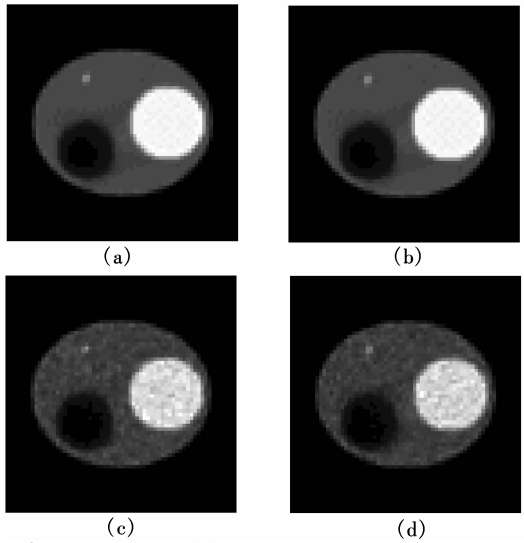

Fig. 2 Reconstructed images. (a) SAGE reconstruction using noise free projections; (b) RBI-SAGE reconstruction using noise free projections; (c) SAGE reconstruction using noise projections; (d) RBI-SAGE reconstruction using noise projections

Fig. 3 displays the log-likelihood versus iteration numbers for the SAGE and RBI-SAGE algorithms. We can observe from Fig. 3 that the log-likelihood of RBI-SAGE increases more rapidly than the log-likelihood of SAGE. Fig. 3 indicates that the RBI-SAGE algorithm converges faster than the SAGE algorithm. We also use the mean absolute error (MAE) and chi-square error (CSE) to evaluate the quality of reconstructed images. The MAE is defined as

$$\varepsilon_{\mathrm{MAE}} = \frac{1}{J}\sum_{j=1}^{J} |x_j^{\mathrm{rec}} - x_j^{\mathrm{org}}| \tag{9}$$

where x_j^{orj} and x_j^{orc} denote the values of pixel j of the original activity image and the reconstructed image, respectively. MAE measures the average discrepancy between the reconstructed image and the original activity image. The CSE is defined as

$$\varepsilon_{\mathrm{CSE}} = \sum_{i=1}^{I} [y_i \log(y_i / \bar{y}_i^{(k)}) - (y_i - \bar{y}_i^{(k)})] \tag{10}$$

$$\bar{y}_i^{(k)} = \sum_{j=1}^{J} p_{ij} x_j^{(k)} \tag{11}$$

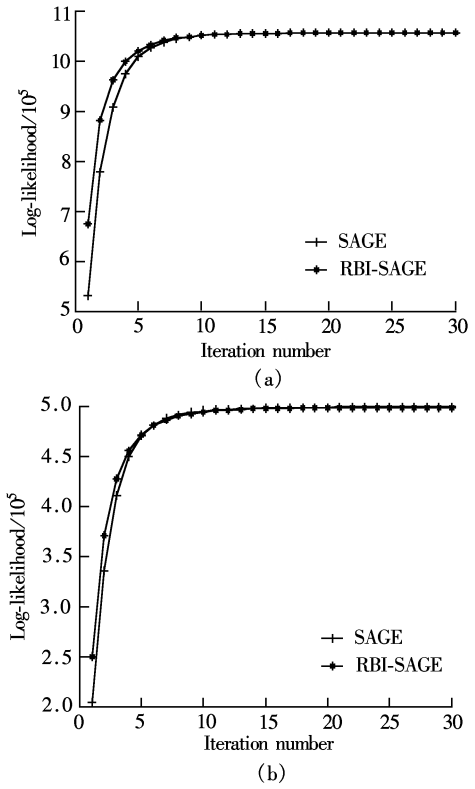

Fig. 3 Comparison of log-likelihood increase versus iteration number k. (a) Projections without noise; (b) Projections with noise

CSE measures the discrepancy between the calculated projections and the original projections. Figs. 4 and 5 display the MAE and CSE values of the reconstructed images using SAGE and RBI-SAGE, respectively. The results show that the MAE and CSE values using RBI-SAGE decrease more rapidly than those obtained with SAGE even if the statistic noise is presented.

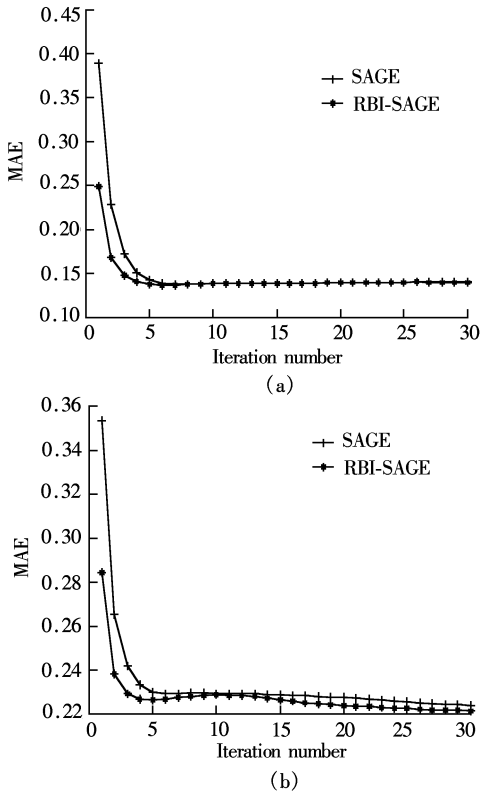

Fig. 4 Mean absolute error of reconstructed images. (a) Projections without noise; (b) Projections with Poisson background noise

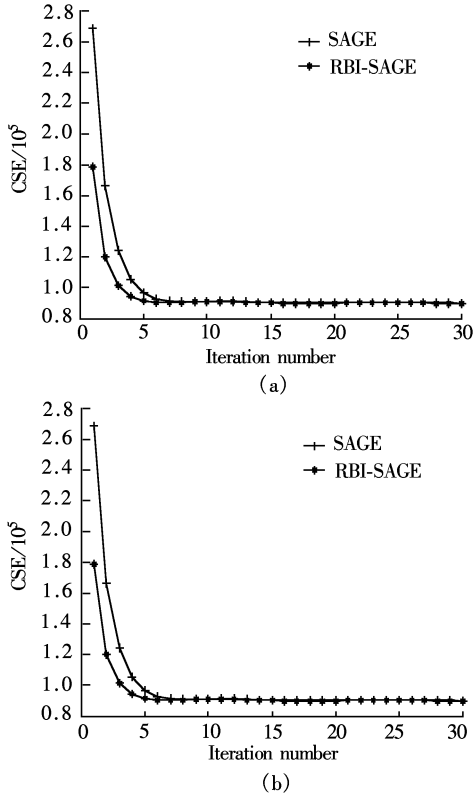

Fig. 5 Chi-square error of reconstructed images. (a) Projections without noise; (b) Projections with Poisson background noise

4 Conclusion

Now, the conventional back projection algorithms are still in use. This is because the EMML algorithm has two main disadvantages: lack of termination criterion and the slow convergence, which impede the practical application of this promising method in the modern PET units. In Ref. [3], Fessler and Hero have proved that the SAGE algorithm easily accommodates smoothness penalties and converges faster than the EMML algorithm. Due to the similarity with the EMML algorithm, ideas used to speed up the EMML algorithm can be used to speed up the SAGE algorithm. Therefore, we have proposed a new approach named RBI-SAGE that combines the RBI algorithm and SAGE algorithm for PET image reconstruction. The experimental results show that the proposed method is superior to the SAGE algorithm.

References

[1] Hudson H M, Larkin R S. Accelerated image reconstruction using ordered subsets of projection data [J]. *IEEE Trans Med Imag*, 1994, **13**(4): 601 – 609.

[2] Byrne C L. Convergent block-iterative algorithms for image reconstruction from inconsistent data [J]. *IEEE Trans Imag Proc,* 1997, **6**(9): 1296 – 1304.

[3] Fessler J A, Hero A O. Space-alternating generalized expectation-maximization algorithm [J]. *IEEE Trans Sig Proc*, 1994, **42**(10): 2664 – 2676.

[4] Fessler J A, Hero A O. Penalized maximum-likelihood image reconstruction using space-alternating generalized EM algorithms [J]. *IEEE Trans Imag Proc*, 1995, **4**(10): 1417 – 1429.

[5] Shepp L A, Vardi Y. Maximum likelihood estimation for emission and tomography [J]. *IEEE Trans Med Imag*, 1982, **MI-1**(2): 113 – 121.

[6] Lalush D S, Tsui B W. Fast transmission CT reconstruction for SPECT using a block-iterative algorithm [J]. *IEEE Trans Nuclear Science*, 2000, **47**(3): 1123 – 1129.

[7] Byrne C L. Likelihood maximization for list-mode emission tomographic image reconstruction [J]. *IEEE Trans Med Imag,* 2001, **20**(10): 1084 – 1092.

[8] Fessler J A, Hero A O. New complete-data spaces and faster algorithms for penalized-likelihood emission tomography [A]. In: *Proceedings of IEEE Conference on Nuclear Science Symposium and Medical Imaging* [C]. Virginia, 1994. 1897 – 1901.

[9] Fessler J A, Hero A O. Complete-data spaces and generalized EM algorithms [A]. In: *Proceedings of IEEE International Conference on Acoustics, Speech, and Signal Processing* [C]. Minneapolis, USA, 1993. 1 – 4.

基于可调子块迭代的加速 SAGE 算法在 PET 图像重建中的应用

朱宏擎　舒华忠　周　健　罗立民

(东南大学生物科学与医学工程系, 南京 210096)

摘要: 提出了一种可调子块迭代(RBI)方法加速空间交替广义期望最大(SAGE)算法的收敛性. 新的可调子块迭代的空间交替广义期望最大算法(RBI-SAGE)组合了 RBI 算法和 SAGE 算法的优点用于加速正电子发射断层(PET)图像重建. RBI-SAGE 将投影数据分成不连续的子块, 每一次迭代仅包含一个这样的子块. 在每一个子块中用 SAGE 算法序列更新参数. 实验中, 运用 RBI-SAGE 算法与 SAGE 算法对 PET 图像进行重建. 结果表明, RBI-SAGE 收敛性能比 SAGE 算法优越, 且重建图像质量较高.

关键词: 正电子发射断层显像; 空间交替最大期望算法; 图像重建; 可调子块迭代; 最大似然

中图分类号: R817